Evidence for two active branches for electron transfer in photosystem I

Mariana Guergova-Kuras*, Brent Boudreaux†, Anne Joliot*, Pierre Joliot*, and Kevin Redding†‡

*Institut de Biologie Physico-Chimique, Centre National de la Recherche Scientifique, UPR 1261, 13 Rue Pierre et Marie Curie, 75005 Paris, France; and †Departments of Chemistry and Biological Sciences and Coalition for Biomolecular Products, University of Alabama, 120 Lloyd Hall, 6th Avenue, Tuscaloosa, AL 35487

Contributed by Pierre Joliot, February 16, 2001

All photosynthetic reaction centers share a common structural theme. Two related, integral membrane polypeptides sequester electron transfer cofactors into two quasi-symmetrical branches, each of which incorporates a quinone. In type II reaction centers [photosystem (PS) II and proteobacterial reaction centers], electron transfer proceeds down only one of the branches, and the mobile quinone on the other branch is used as a terminal acceptor. PS I uses iron-sulfur clusters as terminal acceptors, and the quinone serves only as an intermediary in electron transfer. Much effort has been devoted to understanding the unidirectionality of electron transport in type II reaction centers, and it was widely thought that PS I would share this feature. We have tested this idea by examining *in vivo* kinetics of electron transfer from the quinone in mutant PS I reaction centers. This transfer is associated with two kinetic components, and we show that mutation of a residue near the quinone in one branch specifically affects the faster component, while the corresponding mutation in the other branch specifically affects the slower component. We conclude that both electron transfer branches in PS I are active.

Upon excitation of the photosystem (PS) I primary donor (P_{700}), an electron is transferred to the primary acceptor, A_0 (a chlorophyll *a* molecule) and in less than 100 ps to a secondary acceptor, A_1, identified as a phylloquinone. From A_1, the electrons are transferred to an iron-sulfur cluster, F_X, and then to the terminal iron-sulfur acceptors, F_A and F_B, which are bound by the extrinsic PsaC polypeptide (1) (see Fig. 1*a*). The structure of PS I at 4-Å resolution (2) revealed the existence of two sets of redox cofactors between P_{700} and F_X, bound with an almost perfect symmetry by the two largest subunits, PsaA and PsaB. Due to this symmetry, the obvious similarity of the PsaA and PsaB polypeptides (≈45–50% identical throughout their length; ref. 3) and the fact that the bacterial type I reaction centers are homodimers (4, 5), the possibility of two parallel electron transfer pathways up to F_X should be considered. However, based on the structural analogies of the core of PS I to the purple bacteria reaction center, which suggested a common evolutionary origin for all photosynthetic reaction centers (6), it has been generally thought that electron transport in PS I is unidirectional, as it is in the type II reaction centers. Most data supporting this view comes from electron paramagnetic resonance (EPR) experiments, in which only a single quinone anion radical can be accumulated during strong illumination under reducing conditions sufficient to reduce the terminal acceptors (7, 8) (although see ref. 9). However, these extreme conditions may well bias the results. Transient EPR experiments under conditions of forward electron transport would be preferable (10, 11), but this technique may lack the time resolution required to observe very fast events. Using visible spectroscopy both forward electron transfer from A_1^- to F_X (12, 13), and charge recombination between P_{700}^+ and A_1^- (14) have been shown to be biphasic. The biphasic oxidation of A_1^- in isolated PS I centers initially was interpreted as reflecting a low equilibrium constant between A_1 and F_X (Fig. 1*b*), leading to a fast (≈25 ns) redox equilibration of A_1 and F_X and a slower (≈150 ns) decay of this quasi-equilibrium state associated with electron transfer from F_X to F_A/F_B (12). Based on the lack of sensitivity of these kinetics to the membrane potential, this model was recently challenged and alternative hypotheses were proposed (13): if there is only one active branch, then there must be two populations of PS I in equilibrium that differ structurally to give rise to different kinetics (Fig. 1*c*). Alternatively, the existence of two active branches would explain the biphasic kinetics as transfer from the two different quinones, one of which is primarily bound by PsaA and the other by PsaB (Fig. 1*d*).

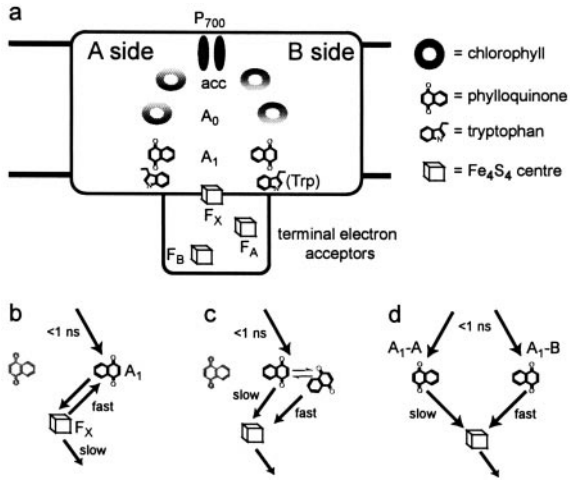

Fig. 1. (*a*) Scheme of cofactor arrangement in PS I. P_{700} is a pair of chlorophylls that serves as the primary electron donor. The accessory (''acc'') and A_0 chlorophylls are both single chlorophyll molecules; A_0 is known to serve as an intermediate in electron transfer, but the role of the accessory chlorophyll in this transfer is still not clear (1, 2). A_1 is a phylloquinone. F_X, F_A, and F_B are 4Fe-4S clusters. Trp represents the tryptophan near the phylloquinone that has been mutated in this study. (*b–d*) Different models to explain the biphasic kinetics of $A_{1(A)}^-$ reoxidation. (*b*) Only one branch is active. A rapid equilibrium is established between A_1 and F_X, which is depleted by forward electron transfer to F_A/F_B. (*c*) Only one branch is active, but the phylloquinone can exist in one of two possible conformations, which may be in equilibrium (slow on the time scale of electron transfer). (*d*) Both branches are active, but the two phylloquinones are in slightly different environments, giving rise to different kinetics of electron transfer to F_X.

Because the understanding of the origin of the biphasic kinetics could give new insights in the electron transport mechanism in PS I, we examined the quinone reoxidation in site-directed mutants of PsaA and PsaB in the genetically tractable

Abbreviations: EPR, electron paramagnetic resonance; F_X, F_A, and F_B, iron-sulfur clusters of photosystem I; PS, photosystem; P_{700}, primary electron donor in PS I; A_0, primary electron acceptor in PS I (chlorophyll); A_1, secondary electron acceptor in PS I (phylloquinone).

‡To whom reprint requests should be addressed. E-mail: Kevin.Redding@mail.ua.edu.

The publication costs of this article were defrayed in part by page charge payment. This article must therefore be hereby marked "*advertisement*" in accordance with 18 U.S.C. §1734 solely to indicate this fact.

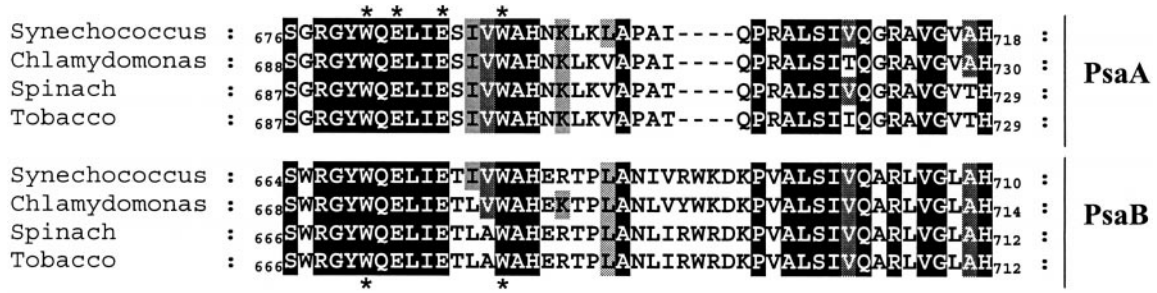

Fig. 2. Sequence alignment of PsaA and PsaB in the region of the n/n′ helix. Asterisks indicate the position of the residues mutated in this work. Conservation profile is color coded for identity (black, 100%; dark gray, 80%; light gray, 60%).

alga *Chlamydomonas reinhardtii.* The data presented here show that mutations introduced in the environment of each phylloquinone specifically alter the two phases of electron transfer from A_1^-. These observations lead to the conclusion that, unlike the situation in the purple bacteria reaction center, both electron transfer branches in PS I are active.

Materials and Methods

Mutant Strains of *C. reinhardtii.* The single mutants were created by bio-ballistic transformation of appropriate gene deletion strains with plasmids containing the point mutations in *psaA* or *psaB*, followed by selection for the linked antibiotic-resistance marker (15). The plasmids in which the mutations were constructed contain the entire *psaB* gene or *psaA* third exon along with flanking sequences to direct recombination and a coinserted *aadA* gene, which serves as a selectable marker. The PsaA–W693F mutation converts codon 693 from TGG (Trp) to TTC (Phe) and was made in plasmid pKR154 (15). The PsaB–W673F mutation was made in plasmid pKR164 (15) and converts codon 673 from TGG to TTC. It also changes codon 674 from CAA (Gln) to CAG (Gln); this silent change introduces a *Bst*NI site used to detect the mutation during cloning.

For kinetic analysis, the recipients were KRC51–3A (*cbn1–48 FUD7 psaA*Δ*)* or KRC52–8A (*cbn1–48 FUD7 psaB*Δ). The FUD7 genotype corresponds to a *psbA* deletion that prevents accumulation of PS II (16) whereas the *cbn1–48* mutation leads to a chlorophyll *b*-less mutant with a reduced amount of light-harvesting complexes (17). The control strain was made by transformation of KRC51–3A with plasmid pKR154, encoding wild-type *psaA-3*. Double mutants were made by cotransformation with both *psaA* and *psaB* plasmids, followed by a genetic cross with KRC62–16A (*mt*$^-$ *cbn1–48 nac2–26 psaA*Δ*psaB*Δ) to generate a *cbn1 nac2* strain (the *nac2* mutation prevents PS II accumulation; ref. 18) harboring both mutations.

Optical Spectroscopy. Spectroscopic measurements on whole cells of *C. reinhardtii* were performed by using a home-built spectrophotometer where absorption changes were probed by using short monochromatic flashes. In the 425- to 500-nm spectral range, the pulses were produced by a Nd:Yag pumped optical parametric oscillator Quanta-Ray MOPO-710 (Spectra-Physics) and in the 375- to 420-nm range by a frequency doubler accessory device FDO-900 (Spectra-Physics). The sample was excited at 700 nm by a tunable dye-laser pumped by the second harmonic of a Nd:Yag laser. The high signal-to-noise ratio of the spectrophotometer (10^5) when using samples with high optical densities such as cell suspensions and the time resolution (5 ns) of the technique have been described (19). *C. reinhardtii* cells were grown in Tris-acetate-phosphate medium (20) at 25°C under low light (6 $\mu E \cdot m^{-2} \cdot s^{-1}$). For spectroscopic measurements the cells were resuspended in 20 mM Hepes (pH 7.2) containing 20% (wt/vol) Ficoll, as well as 5 μM carbonyl cyanide (4-(trifluoromethoxy)phenyl)hydrazone to collapse the permanent transmembrane potential. The dependence of the flash-induced absorption changes at 430 and 380 nm upon the energy of the actinic flash was measured for each strain. Kinetics measurements were performed with light energies just sufficient to saturate the signal at 380 nm. When significantly higher actinic energies were used, we observed an additional fast decay component ($\tau < 5$ ns) at 430 nm in all strains. The decay-associated spectra of the kinetic phases were obtained from a global analysis of the individual kinetics obtained at each wavelength, using the MEXFIT program (21).

Results

The mutations in PsaA and PsaB were designed by using the crystal structures of PS I and the related purple bacterial reaction center as a guide (2, 6, 22). The structural data on PS I suggested that the most likely region for binding the phylloquinones was the stretch of highly conserved residues in PsaA and PsaB forming the stromal α-helices n and n′ (2). Additionally, magnetic resonance data indicated that an aromatic nitrogen-containing amino acid was close to the phylloquinone A_1^- radical (23). We have introduced site-directed mutations in the tryptophan and histidine residues conserved between PsaA and PsaB in this region (Fig. 2) and found that mutation of Trp-693 in the PsaA (PsaA–W693F) polypeptide specifically disturbed the A_1^- EPR spectrum (B.B., F. MacMillan, C. Teutloff, K. Brettel, F. Gu, S. Grimaldi, R. Bittl, and K.R., unpublished work). Here we examine the effect of the conversion of these tryptophans (PsaA–W693 and PsaB–W673) to phenylalanines upon the *in vivo* kinetics of A_1^- reoxidation. We also constructed a double mutant that contains both point mutations (PsaA–W693F/PsaB–W673F). Three additional mutants were examined: two single substitutions of the conserved glutamates 695 and 698 in PsaA for glutamines (mutants PsaA–E695Q and PsaA–E698Q) and a double mutant in which the two tryptophans further along the n/n′ helices (Fig. 2) were modified to phenylalanines (PsaA–W702F/PsaB–W682F). All single mutations as well as the double mutations did not prevent photoautotrophic growth of the mutant strains under either aerobic or anaerobic conditions (data not shown). To simplify the spectroscopic and kinetic analysis, we introduced these mutations into a control strain lacking PS II and chlorophyll *b*.

Transient absorption signals in the nanosecond-microsecond time scale were recorded at discrete wavelengths in the 370- to 500-nm spectral range after selective laser flash excitation (700 nm) of PS I in the control strain. Global analysis of the data resolved four components: three exponential decays (two in the nanosecond and one in the microsecond time range) and a component that did not decay on the detection time scale (30 μs). The spectrum of the nondecaying component was associated with the electrochromic shifts due to the flash-induced delocalized membrane potential. The spectrum had a positive peak at

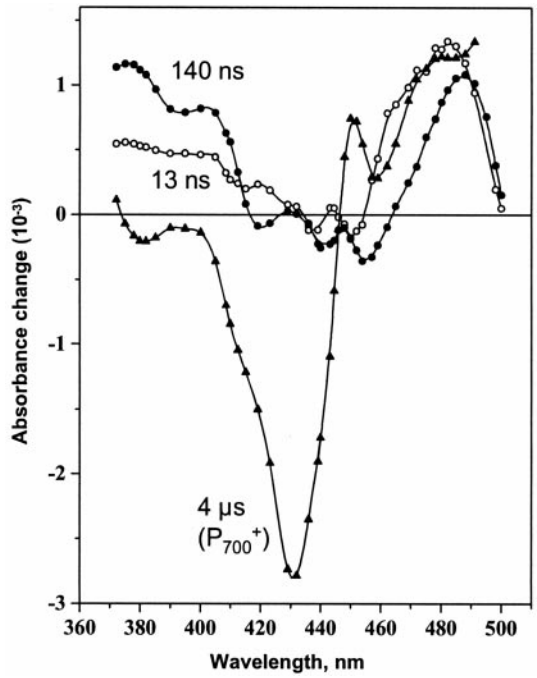

Fig. 3. Decay associated spectra of the 13 ns (○), 140 ns (●), and 4 μs (▲) components, obtained from global analysis of transient absorption data in whole cells of the *C. reinhardtii* control strain. Flash-induced kinetics in the 5 ns-30 μs time range were measured at each wavelength to obtain the three exponential components. Deconvolution with more exponential components did not improve the results.

475 nm and negative peaks at 490, 460, and 420 nm, characteristic for the pigment electrochromic changes in mutants lacking chlorophyll *b* (24). The spectra of the three exponential decays are shown in Fig. 3. The microsecond component was assigned to P_{700}^+ reduction, based on the typical bleaching at 430 nm (25) and a half-time of 4 μs characteristic of its reduction by plastocyanin in intact algae (26). The spectra of the two nanosecond phases were attributed to reoxidation of A_1^-. As previously observed in cyanobacteria (27) and *Chlorella* (13), the nanosecond phases displayed positive absorption in the 370- to 400-nm range, characteristic for semiphylloquinone, and contributions from the electrochromic band shifts induced by the presence of a charge on A_1. The positive band at 480 nm has been attributed to a shift in the absorption spectrum of a carotenoid molecule in the close vicinity of the phylloquinone. It should be noted that the two decay-associated spectra exhibited subtle but significant differences in shape in the near-UV region (371–410 nm) and more obvious differences above 410 nm. The half-times (13 and 140 ns) and spectra of the two nanosecond decays were similar to those seen in *Chlorella* (13). In the case of *Chlorella*, two differences should be noted, a slightly slower half-time of the fast phase (20 ns compared with 13 ns) and almost equivalent absorption at 380 nm for the two nanosecond decays. Thus, biphasic kinetics of electron transfer from A_1 to F_X are also present in *Chlamydomonas* PS I and may well be a universal feature.

The P_{700}^+ re-reduction was followed at 430 nm in all mutant strains, and the kinetics could be well fit by a single exponential with a half-time of ≈4 μs (Table 1). We did not observe absorption changes at this wavelength in the tens of nanoseconds time range, where charge recombination in the primary pair $P_{700}^+ A_0^-$ would occur (1). This indicated that the mutations did not prevent electron transfer up to A_1.

To examine the effects of the mutations on electron transfer from A_1 to F_X, we measured the kinetics of the absorption decay at 380 nm, in the semiphylloquinone absorption band, where contributions from P_{700}^+ reduction and electrochromic shifts are small. The results for the two symmetric mutants PsaA–W693F and PsaB–W673F and the double mutant containing both mutations (PsaA–W693F/PsaB–W673F) are shown in Fig. 4. The mutation of the tryptophan in PsaA affected specifically the kinetics of the slow nanosecond component, increasing its half-time from ≈140 ns to ≈490 ns. The rate constant of the fast component and the ratio between the amplitudes of the two phases were the same as in the control strain (Fig. 4*a*; Table 1). Mutation of the corresponding tryptophan in PsaB (PsaB–W673F) slowed the initial part of the kinetics but did not modify the later part, which is clearly seen in the conformity of the latter part of the traces (Fig. 4*b*). In the double mutant (PsaA–W693F/PsaB–W673F), the overall kinetics were retarded and two distinct phases were well resolved (Fig. 4*c*), a slow one with the same half-time as in the single PsaA–W693F mutant (≈490 ns) and a faster one with a half-time of ≈73 ns (Table 1). The kinetics in the PsaB–W673F mutant could be fit poorly with a single exponential component ($t_{1/2}$ = 110 ns). However, the fit was significantly better if we assumed that two components were still present in the kinetics of A_1^- reoxidation and constrained the half-times of the two components to match the modified fast

Table 1. Kinetic parameters of electron transfer in the mutant strains

	A_1^- oxidation					
	Fast phase		Slow phase		Amplitude*	P_{700}^+ reduction,
Strain	$t^{380\ nm}$ (ns)	$t^{480–457\ nm}$ (ns)	$t^{380\ nm}$ (ns)	$t^{480–457\ nm}$ (ns)	(% of total)	$t^{430\ nm}$ (μs)
Control	13 ± 2	13 ± 3	143 ± 10	160 ± 11	34 ± 3	4.0 ± 0.2
PsaA–W693F	15 ± 2	12 ± 3	**490 ± 21**	**355 ± 120**	34 ± 2	4.0 ± 0.2
PsaB–W673F	**73**†	**62**†	143†	160†	33 ± 10	4.2 ± 0.3
W693F/W673F	**73 ± 17**	**62 ± 28**	**485 ± 70**	**350 ± 100**	49 ± 9	4.1 ± 0.2
PsaA–E695Q	11 ± 5	n.d.	**277 ± 33**	n.d.	44 ± 11	4.4 ± 0.3
PsaA–E698Q	11 ± 4	n.d.	**222 ± 30**	n.d.	36 ± 10	3.9 ± 0.2
W702F/W682F	19 ± 12	n.d.	187 ± 28	n.d.	n.d.	3.9 ± 0.2

The half-times (*t*) were estimated from the data using fits to one or two exponential decay components. The measurement at 380 nm is in the spectral region of the semiphylloquinone absorption, the difference 480–457 nm is in the electrochromic band shift induced by the presence of charge on A_1. The half-time of P_{700} re-reduction was calculated from the decay of the absorption change at 430 nm. n.d., not determined.

*The relative amplitude of the fast nanosecond phase expressed as percentage of the total amplitude was estimated from the kinetics at 380 nm. Values that are significantly different from those of the control strain are in bold.

†The half-times of the two phases used to fit the data for PsaB–W673F strain were fixed parameters with values taken from the double mutant for the fast phase and from the control strain for the slow phase, as described in the text.

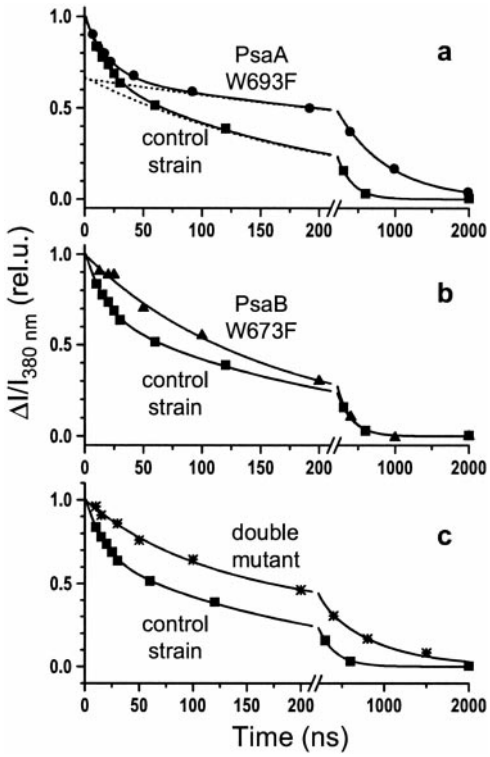

Fig. 4. Kinetics of $A_{1(A)}^-$ oxidation measured at 380 nm for the control strain (■), PsaA–W693F mutant (●), PsaB–W673F mutant (▲), and the PsaA–W693F/PsaB–W673F double mutant (*). The solid lines are theoretical fits with the parameters shown in Table 1. The dotted lines are the extrapolation of the slow phase to show its amplitude in the control strain and the PsaA–W693F mutant strain.

phase found in the double mutant and the slow phase of the wild type (73 ns and 140 ns, Table 1). The combined results of the kinetics deconvolution with all parameters free in the double mutant and the constrained fit for the single mutant PsaB–W673F showed that the fast phase (≈13 ns) of A_1^- reoxidation was specifically affected by mutation of the tryptophan W673 in PsaB polypeptide. Similar values also were obtained when the electrochromic band shift (480–457 nm) was used as a reporter of A_1^- reoxidation (Table 1).

Mutation of the residues Glu-695 and Glu-698 in PsaA affected specifically the kinetics of the slow phase although to a much smaller extent than in the PsaA–W693F mutant (Table 1). Both glutamates are located on the stromal helix a few residues from Trp-693, and it has been suggested that their negatively charged side chains could contribute to lowering the redox potential of the phylloquinone (23). The kinetics of A_1^- reoxidation in the double mutant PsaA–W702F/PsaB–W682F, where the conserved tryptophans located further along the stromal helix n/n′ were modified to phenylalanines, were not significantly different from the control strain (Table 1). This indicated that the effects observed upon mutation of the Trp-693/Trp-673 pair are related to their proximity to the phylloquinones and their specific interaction.

Fig. 5 compares the spectral features of the two nanosecond decay components collected in the semiphylloquinone absorption region for the control strain, PsaA–W693F, and the double mutant PsaA–W693F/PsaB–W673F. Globally the fast component in the control strain had relatively flat spectrum between 380 and 405 nm whereas the spectrum of the slow component presented two bands with different intensities, one at ≈380 nm and the other at ≈400 nm, the ratio between them ≈1.4. In the PsaA–W693F mutant the spectrum and the half-time of the fast component (17 ns) were similar to the control strain. Interestingly, in the spectrum of the slow component the position of the two bands were not modified but the ratio between them decreased to ≈1.1. Thus the mutation in PsaA not only slowed down the slow phase of A_1^- reoxidation but modified its spectral properties. This modified spectrum, with a ratio $\Delta A_{380}/\Delta A_{400}$ of ≈1.1 is seen again in the double mutant. Moreover, the spectrum of the retarded fast decay is also changed with a net absorption increase at 400 nm. We could therefore attribute the similar spectral modification (decrease of the ratio $\Delta A_{380}/\Delta A_{400}$) to the mutation of PsaB–Trp-673 to phenylalanine.

Discussion

In this work we have studied the reoxidation kinetics of A_1^- in whole cells of the green algae *C. reinhardtii*. The spectra and kinetics associated with phylloquinone reoxidation in *C. reinhardtii* were similar to other green algae (13). We found that the two kinetic components of A_1^- reoxidation can be modulated independently and specifically by mutating Trp-693 in PsaA or Trp-673 in PsaB. The fact that mutation of the tryptophans PsaA–W702 and PsaB–W682, which are located at the end of the stromal helices n/n′, had no effect upon phylloquinone reoxidation indicates that they are not in the proximal environment of the phylloquinones. This is consistent with recent high-resolution crystallographic data showing that both PsaA–W693 and the symmetry-related PsaB–W673 are in contact with the phylloquinones on their respective side (P. Jordan, P. Fromme, and N. Krauß, personal communication). Therefore, we con-

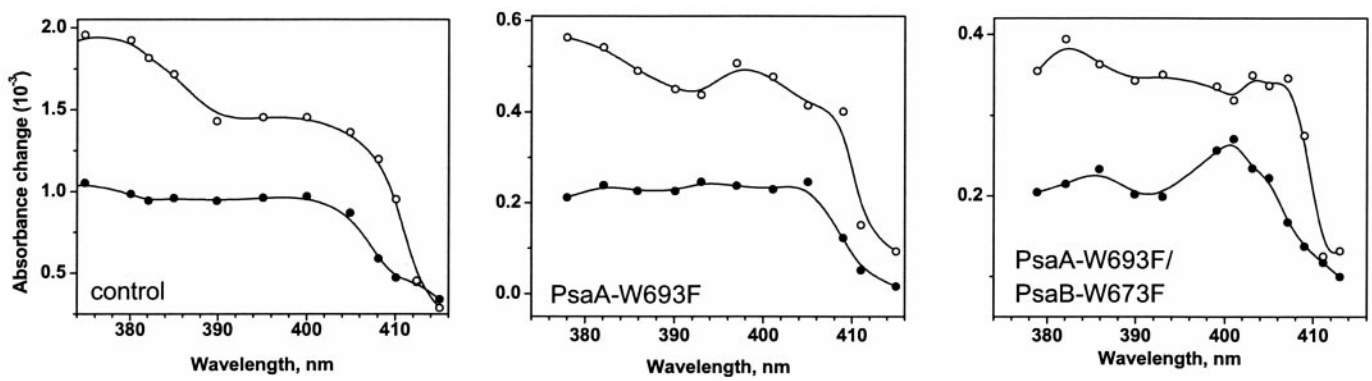

Fig. 5. Comparison of the spectra of the two nanosecond decay components in the region of semiphylloquinone absorption in the control strain (*Left*), PsaA–W693F (*Center*), and PsaA–W693F/PsaB–W673F (*Right*) mutants. The amplitudes of the components at the probe wavelengths, where the kinetics were measured, are shown as symbols. Closed symbols are the spectra of the fast phase, open symbols are the spectra of the slow phase.

clude that both quinones can be reduced by PS I photochemistry and that both are reoxidized by F_X. Furthermore, we can assign the fast (≈13 ns) component to the reoxidation of the phylloquinone on the PsaB side and the slow (≈140 ns) component to the reoxidation of the phylloquinone on the PsaA side. The implication of these results is that electron transfer in PS I, unlike type II reaction centers, is bi-directional.

Our results strongly argue against both of the models that use a single active branch. In the equilibrium model (Fig. 1*b*), it is not possible to change the rate of only one of the phases while keeping the other rate and the ratio between the phases constant. Likewise, the structural heterogeneity model (Fig. 1*c*) would predict that mutation of one of the tryptophans (the one next to the "inactive quinone") would have no effect on either phase. Mutations can exert effects over relatively long distances, and one might invoke such indirect effects to explain the phenotype of the mutation near the inactive quinone. However, this would require a complex reasoning: a mutation near the active quinone would have a direct effect upon it (modifying the spectrum of the semiquinone and slowing its rate of oxidation) only when the reaction center is in one conformation but not in the second; at the same time, a mutation on the other side would act over a relatively long distance to exert the exact same kind of effect on the active quinone, but only when in the second conformation. Therefore, we favor the simplest interpretation of our data, which is that charge separation can proceed down either branch (Fig. 1*d*). We should make clear that our data do not directly examine initial charge separation. However, if one posits that this event were biased to a unique branch to produce a specific $P_{700}^{+}A_{0}^{-}$ state, then one must explain the reduction of the phylloquinone on the other branch. A_1 is reduced faster than the resolution time of our instrument (5 ns), consistent with previous reports for A_0 reoxidation with a half time of a few tens of picoseconds (28). Electron transfer between the two phylloquinones, based on the distance between them (22.3 Å; ref. 2) and the "Moser-Dutton ruler" (29), would be slower than 10 ms, which is several orders of magnitude slower than A_1 reoxidation. In a similar fashion we can rule out electron transfer across branches at the level of A_0 based on the distances. The distance between eC3 and eC3′ in the PS I structure is 26.5 Å (2) and the distance from A_0 to the phylloquinone on the other branch is even longer.

Thus, we conclude that the initial excited state P_{700}^{*} can evolve into either $P_{700}^{+}A_{0(A)}^{-}$ or $P_{700}^{+}A_{0(B)}^{-}$ states, with $A_{0(A)}$ and $A_{0(B)}$ representing the analogous chlorophyll of the A or B branch, respectively. Secondary electron transfer events (in the picosecond time scale) then would lead to the states $P_{700}^{+}A_{1(A)}^{-}$ or $P_{700}^{+}A_{1(B)}^{-}$. The next stage, which is the one that we observe in this study, is the tertiary electron transfer leading to the singular state $P_{700}^{+}F_{x}^{-}$. Theoretically, we could estimate the contribution of electron transfer down each branch by the relative amplitude of each kinetic phase. If the amplitude of the spectral changes associated with the reoxidation of the two phylloquinones were identical, then we would estimate that electrons are partitioned between each branch with a preference (55–66%) for the one leading to the quinone on the PsaA side. However, these numbers should not be considered rigorous, as the spectra displayed some dissimilarity that could be interpreted as differences in the local environment of each phylloquinone and/or different contributions of the electrochromic band shifts. Some of these differences may be explained by new crystallographic data, which reveal that the proximity and orientations of the carotene(s) nearest to the phylloquinone on either side are significantly different (P. Jordan, P. Fromme, and N. Krauß, personal communication).

It is worth noting that mutation of each tryptophan had a similar effect on the quinone close to it. In both cases, conversion to a phenylalanine had two effects on one of the kinetic phases: a modification of the decay-associated spectrum and a 3- to 5-fold decrease in the rate of its decay. The spectral change was also similar in both cases, manifesting itself as an increase in absorbance at ≈400 nm. Two possible explanations that are not mutually exclusive could be given for this change: (*i*) Because the Trp residues (PsaA–Trp-693 and PsaB–Trp-673) are involved in a π-stacking interaction with the phylloquinones, as previously suggested based on electron spin echo envelope modulation spectroscopy (23), their mutation to Phe will likely perturb the electron coupling between the quinone ring and the aromatic side chain leading to a different absorption properties of A_1. (*ii*) The mutation could lead to a change in the local environment of the phylloquinone, and thus to slightly different interactions with the neighboring chromophores, most probably chlorophylls, modifying the electrochromic bandshifts.

The change in the rate of electron transfer (k_{et}) from the quinone to F_X in the mutant strains can be easier to explain in the context of the empirical equation derived by Moser *et al.* (29)

$$\log k_{et} = 15 - 0.6R - 3.1(\Delta G_0 + \lambda)^2/\lambda,$$

where R is the edge-to-edge distance between A_1 and F_X in Å, and ΔG_0 and λ are the standard free energy and the reorganization energy of the reaction, respectively. One or more of the terms in this equation could have been modified in the mutant strains. It is possible that the altered phylloquinone-binding site causes a slight increase in the distance between the quinone and F_X and/or orientation of the quinone. A 3–5 time decrease in the rate of electron transfer would correspond to an increase of ≈0.9 Å in R if all other parameters were constant. Similarly the mutation can lead to an increase of either ΔG_0 or λ, and thus result in a lower rate of electron transfer. The unusually low midpoint potential of A_1/A_1^{-} has been attributed to its very hydrophobic environment and/or specific interactions with the phylloquinone in PS I (30). Modification of either or both may occur when the indole ring system of the Trp is exchanged for the smaller phenyl side chain of Phe. The π-stacking interaction of the side chain to the quinone could have been perturbed or the binding site rendered more exposed to aqueous solvent. This would tend to stabilize the semiquinone radical anion, thus decreasing driving force, and force the movement of nearby polar molecules in response to the change in charge during electron transfer, thus increasing the reorganization energy. If the nearby conserved glutamates (695/675 and 698/678) are deprotonated, then their negative charge might contribute to this effect, and conversion to the uncharged glutamine would stabilize the semiquinone anion and slow the rate of transfer to F_X. We did observe ≈2-fold and ≈1.5-fold decreases in the rate of reoxidation of $A_{1(A)}^{-}$ upon mutation of the nearer (Glu-695) and farther (Glu-698) glutamic acid residues of PsaA, lending support to this idea. However, these modest changes may indicate that these carboxylates may be either relatively far from the quinone or at least partially shielded by counter ions.

Reasoning similar to that above can be applied to explain the difference in the rate of reoxidation of $A_{1(B)}^{-}$ as compared with that of $A_{1(A)}^{-}$. However, a difference in the distance between the two quinones and F_X seems less likely because an order of magnitude faster rate would require 1.7-Å shorter distance on the PsaB branch. All available structural data indicate equivalent positions for both quinones with respect to the symmetry axis and thus to F_X (2). Therefore we would tend to attribute the difference in rate to a difference in the amino acid compositions of the two phylloquinone sites. To that end, we are now examining mutations in several conserved amino acids (such as tryptophans and glutamates) that are not shared between PsaA and PsaB.

The presence of bi-directional electron transfer to quinones in slightly different environments, leading to unequal rates of

transfer to the next cofactor immediately begs the question: what, if any, is the functional significance of this arrangement? Because the primeval reaction center was almost certainly homodimeric (discussed in refs. 3 and 31), and this situation persists in PS I's cousins found in green sulfur bacteria (5) and heliobacteria (4), it is likely that the original mode of electron transfer was bi-directional. The heterodimeric type II reaction centers, which use one quinone (Q_A) as a secondary acceptor (like A_1) and the other (Q_B) as a terminal acceptor, have evolved to eliminate electron transfer directly to Q_B. Thus, Q_A serves as a "one-electron gate," while Q_B is doubly reduced, and electron transfer from Q_A to Q_B is coupled to protonation of Q_B to the quinol form, an essential part of its function. In contrast, no such selection pressure was necessary in type I reaction centers, where the semiquinone on one branch donates its electron to a cofactor that sits in the symmetry axis, and it makes no difference from which side it came. Reduction of ferredoxin by PS I is limited by electron transfer from the iron-sulfur clusters, and therefore the slower rate from $A_{1(A)}^-$ to F_X ($t_{1/2} \approx 140$ ns) would not restrict overall electron transfer. We also should note that the PsaB–W673F mutant, in which the rates of electron transfer from the two phylloquinones to F_X are almost equivalent, shows no observable defects in photosynthesis *in vivo* and is indistinguishable from the wild type. However, because PS I has a large antenna (100 chlorophyll molecules) and the kinetics for $P_{700}^+A_{0)}^-$ formation are on the same time scale as excitation energy transfer (1), the presence of two branches for initial charge separation would double the rate of exciton trapping and thus increase the efficiency of PS I charge separation. Further studies in which the environment of P_{700} and the primary electron acceptor(s) in PsaA and PsaB is modified may help to answer the question of whether or not the existence of two electron transfer pathways has functional implications.

We thank F. Rappaport, R. Kuras, R. Metzger, and D. Oppenheimer for critical reading of the manuscript. K.R. acknowledges support from DuPont through a DuPont Young Professor Grant and the U.S. Department of Energy through an Energy Biosciences Grant. M.G.-K., A.J., and P.J. acknowledge support from the Centre National de la Recherche Scientifique and the Collège de France.

1. Brettel, K. (1997) *Biochim. Biophys. Acta* **1318,** 322–373.
2. Klukas, O., Schubert, W. D., Jordan, P., Krauß, N., Fromme, P., Witt, H. T. & Saenger, W. (1999) *J. Biol. Chem.* **274,** 7361–7367.
3. Golbeck, J. H. (1993) *Proc. Natl. Acad. Sci. USA* **90,** 1642–1646.
4. Liebl, U., Mockensturm-Wilson, M., Trost, J. T., Brune, D. C., Blankenship, R. E. & Vermaas, W. (1993) *Proc. Natl. Acad. Sci. USA* **90,** 7124–7128.
5. Buttner, M., Xie, D. L., Nelson, H., Pinther, W., Hauska, G. & Nelson, N. (1992) *Biochim. Biophys. Acta* **1101,** 154–156.
6. Schubert, W. D., Klukas, O., Saenger, W., Witt, H. T., Fromme, P. & Krauß, N. (1998) *J. Mol. Biol.* **280,** 297–314.
7. MacMillan, F., Hanley, J., van der Weerd, L., Knupling, M., Un, S. & Rutherford, A. W. (1997) *Biochemistry* **36,** 9297–9303.
8. Yang, F., Shen, G., Schlucter, W. M., Zybailov, B. L., Ganago, A. O., Vassiliev, I. R., Bryant, D. A. & Golbeck, J. H. (1998) *J. Phys. Chem. B* **102,** 8288–8299.
9. Heathcote, P., Hanley, J. A. & Evans, M. C. W. (1993) *Biochim. Biophys. Acta* **1144,** 54–61.
10. Sieckmann, I., van der Est, A., Bottin, H., Sétif, P. & Stehlik, D. (1991) *FEBS Lett.* **284,** 98–102.
11. van der Est, A., Bock, C., Golbeck, J., Brettel, K., Setif, P. & Stehlik, D. (1994) *Biochemistry* **33,** 11789–11797.
12. Setif, P. & Brettel, K. (1993) *Biochemistry* **32,** 7846–7854.
13. Joliot, P. & Joliot, A. (1999) *Biochemistry* **38,** 11130–11136.
14. Brettel, K. & Golbeck, J. H. (1995) *Photosynth. Res.* **45,** 183–193.
15. Redding, K., MacMillan, F., Leibl, W., Brettel, K., Rutherford, A. W., Breton, J. & Rochaix, J.-D. (1998) in *Photosynthesis: Mechanisms and Effects*, ed. Garab, G. (Kluwer, Dordrecht, The Netherlands), pp. 591–594.
16. Bennoun, P., Spierer-Herz, M., Erickson, J., Girard-Bascou, J., Pierre, Y., Delosme, M. & Rochaix, J. D. (1986) *Plant Mol. Biol.* **6,** 151–160.
17. Allen, K. D. & Staehelin, L. A. (1994) *Planta* **194,** 42–54.
18. Kuchka, M. R., Goldschmidt-Clermont, M., van Dillewijn, J. & Rochaix, J. D. (1989) *Cell* **58,** 869–876.
19. Béal, D., Rappaport, F. & Joliot, P. (1999) *Rev. Sci. Instrum.* **70,** 202–207.
20. Harris, E. H. (1989) *The Chlamydomonas Sourcebook: A Comprehensive Guide to Biology and Laboratory Use* (Academic, San Diego).
21. Muller, K.-H. & Plesser, T. (1991) *Eur. Biophys. J.* **19,** 231–240.
22. Schubert, W. D., Klukas, O., Krauß, N., Saenger, W., Fromme, P. & Witt, H. T. (1997) *J. Mol. Biol.* **272,** 741–769.
23. Hanley, J., Deligiannakis, Y., MacMillan, F., Bottin, H. & Rutherford, A. W. (1997) *Biochemistry* **36,** 11543–11549.
24. Hildreth, W. W. (1970) *Arch. Biochem. Biophys.* **139,** 1–8.
25. Ke, B. (1972) *Arch. Biochem. Biophys.* **152,** 70–77.
26. Delosme, R. (1991) *Photosynth. Res.* **29,** 45–54.
27. Brettel, K. (1988) *FEBS Lett.* **239,** 93–98.
28. Hastings, G., Kleinherenbrink, F. A., Lin, S., McHugh, T. J. & Blankenship, R. E. (1994) *Biochemistry* **33,** 3193–3200.
29. Moser, C. C., Keske, J. M., Warncke, K., Farid, R. S. & Dutton, P. L. (1992) *Nature (London)* **355,** 796–802.
30. Iwaki, M. & Itoh, S. (1991) *Biochemistry* **30,** 5347–5352.
31. Nitschke, W., Matteoli, T. & Rutherford, A. W. (1996) in *Origin and Evolution of Biological Energy Conversion*, ed. Baltcheffsky, M. (VCH, New York), pp. 177–203.